Monte Carlo Simulation of e^- Detection in a Spark Chamber

Sasha Bakker, Joseph DiStasio, and Douglas Pazitka-Dorado
Physics Department, University of Massachusetts Amherst.
(Dated: December 14, 2020)

ABSTRACT

The Monte Carlo method simulates a physical system though randomized sampling of the parameter space, by scaling by the probability of parameters. Research regrading experimental determination of the Muon mass was performed by Benjamin Brau of the University of Massachusetts Physics Department [1]. In their paper, *experimental data* obtained from a spark chamber was compared to *simulated data* from a Monte Carlo simulation. The resulting muon energy was determined to be 100 ± 5 MeV. To improve upon this simulation, our simulation changes some assumptions about the probability distribution for the angle of the electron's path from the chamber's axis. $Non-uniform$ probability distributions gave the most accurate result when compared to the accepted value for muon energy, 105.7 MeV. The distribution with the lowest χ^2_{min} that falls within uncertainty of the accepted energy, is from a positive-linear angle distribution, with the maximum angle as 30^o, yielding the result for the muon mass: $101.9 \pm 6.0 \frac{\text{MeV}}{c^2}$.

I. INTRODUCTION

Muons are negatively charged subatomic particles that form during the collision between cosmic rays and the nuclei of atmospheric gases. They are classified as leptons and are similar to electrons with the key difference being that the muon mass is significantly larger, with an accepted mass of $105.7 \frac{\text{MeV}}{c^2}$. This difference causes muons to be unstable such that the decay of a free muon is almost guaranteed to decay into an electron, electron antineutrino, and muon neutrino. This reaction is demonstrated below:

$$\mu^- \rightarrow e^- + \overline{\nu_e} + \nu_\mu \tag{1}$$

While the muon mass is generally accepted to be approximately 200 times larger than that of an electron, measuring it can be difficult. A particular method of experimentally calculating the mass is utilizing a spark chamber particle detector and fitting the data taken from it to a Monte Carlo simulation. In this experiment, we take the data from a prior group's and use a Monte Carlo simulation to deduce our best estimate of the muon mass.

II. BACKGROUND

A. Experimental

The experimental basis for this report utilizes a spark chamber, which is a particle detector that in this case is used to detect entering muons. More specifically, we are taking the experimental data from Brau *et al.* [1], and their diagram is depicted in Fig. 1.

Twenty-One circular aluminum plates are layered on top of one another with a characteristic thickness t_g between them - known as the 'spark gap.' Every other plate is charged with some characteristically high voltage. When a muon enters the chamber, it leaves a trail of ionized gas which 'sparks' due to the high electric voltage. The number of sparks produced is the spark number n_s.

The number of spark gaps n_s traversed before being stopped by the chamber's aluminum plates, quantifies the energy of the particle resulting from the muon decay. The charged particle moving within the chamber ionizes noble gas, leaving a path of ionized atoms between the plates. A high voltage supply is supplied across the plates, and the ionized path gives a reduced resistance: this causes sparks to form along this trajectory. In this experiment, the angle of the electron's path from the chamber's axis θ was only recorded to $\theta_{max} \approx 30^o$ for the creation of sparks due to a downward directed electron. The resulting experimental data had 43 muon decay observations as summarized by Table I. To deduce the muon mass from the number of sparks, a Monte Carlo simulation was implemented while varying the energy from 60 MeV to 140 MeV in steps of 5 MeV. The simulation and experimental data were compared by calculating the sum of squared residuals at each energy. The minimum of this quantity occurs at 100 MeV such that the muon mass was found to be $m_\mu = 100 \pm 5 \frac{\text{MeV}}{c^2}$.

Number of Sparks	Number of Muon Decays
3	4 ± 2
4	7 ± 3
5	13 ± 4
6	15 ± 4
7	4 ± 2

TABLE I. The experimental data where $N_{tot,exp} = 43$ and $\theta_{max} = 30^o$ [1].

B. Simulated

A Monte Carlo simulation is a simulated model that is used to find the probability of potential outcomes. In the context of our experiment, we vary multiple parameters to simulate a muon entering the spark chamber. Using these values, we utilize a set of equations that determines the spark number of each entering muon. This simulation (which is explained in detail in section III.B) allows us to compare the different spark number distributions of various muon masses, thus allowing us to calculate the likely muon mass measured in the initial experiment [1].

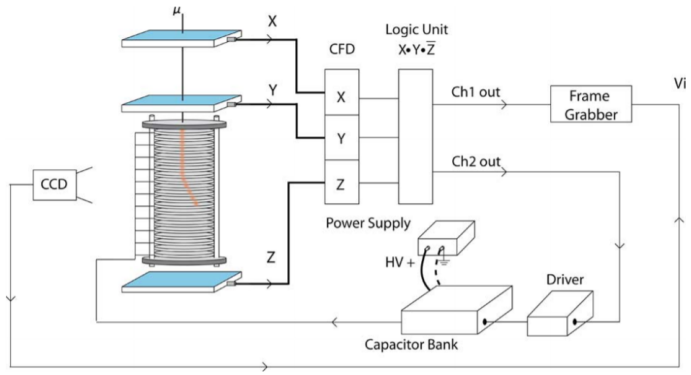

FIG. 1. Apparatus used in experimental trials [1]. Notable parts of it include the spark chamber itself, and electronics used to detect muons, and the image acquisition tool to view images of the muon

III. METHODS

The goal for this experiment is twofold. First, we recreated the simulation referenced in [1] by using the geometrical assumptions and experimental data. Secondly, we modify the simulation by implementing different probability distributions for the angle of the electron's path from the chamber's axis and lowering the step size between energies. This was done in order compute a more accurate muon mass value, compared to its accepted value of $105.7\frac{\text{MeV}}{c^2}$, than the reference measurement of $100 \pm 5\frac{\text{MeV}}{c^2}$. It is important to note that the angle of the electron's path from the chamber's axis had experimental limitations. This is because the Brau group only recorded incoming angles up to 30^o, meaning if there had been sparks past this maximum, the data did not reflect such events. This bound was determined because if the ionized path has too steep, the likely hood of escape before stopping was greatly increased. This is not to say that there were no electrons with paths greater than 30^o; these were simply not experimentally viable for counting the number of sparks produced.

A. Experimental Geometry

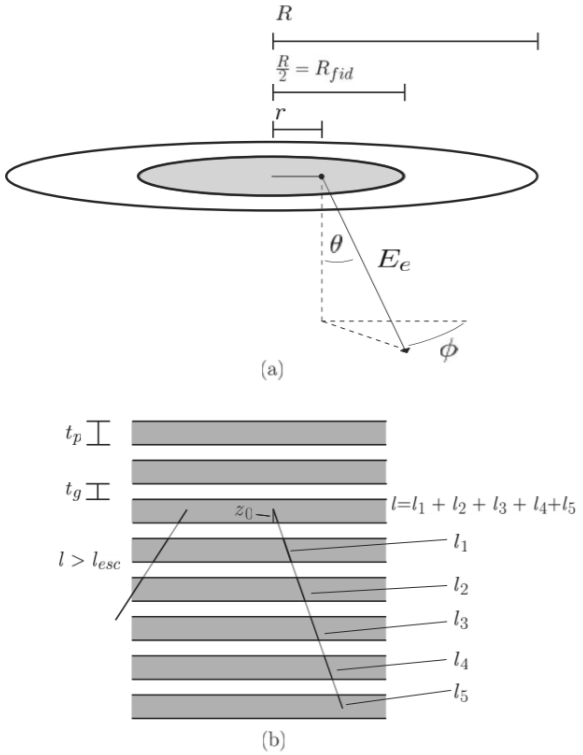

FIG. 2. The spark chamber experimental geometry. (a) The spatial position of the decaying electron with initial kinetic energy E_e at radial distance r with the polar angle θ and the azimuthal angle Φ. (b) The spatial position of the decaying electron inside the chamber is at height z_0, and the electron will traverse the length l, before being stopped by the aluminum.

As seen in Figure 2 part (b), the spark chamber's main component is a cylinder of 21 stacked aluminium plates with thickness $t_p = 0.9525$ cm and radius $R = 7.62$ cm. The plates are separated by spark gaps of thickness $t_g = 0.635$ cm that are filled with Neon, a noble gas. The decay is expected to occur at a distance z_0, orthogonal to the surface of the plate, with a path length l (Eq. 3) until stopped by the aluminum. Sparks will form along the trajectory, in the gaps between the plates. Correspondingly, the electron will have an escape length l_{esc} such that if $l > l_{esc}$ (Eq. 4), the electron will escape the chamber before it is stopped. As seen in Figure 2 part (a), the electron is assumed to be located at a radial distance r less than the radius of the fiducial volume $R_{fid} = \frac{R}{2}$ from the chamber's axis. Its initial velocity will be in the downward direction at the polar angle θ and azimuthal angle Φ relative to the chamber's axis.

The electron's initial kinetic energy in the spark chamber E_e is slowed during its travel through aluminum. Ionization is the dominant energy-loss process for the electron such that there is a critical energy $E_{crit} = S_0 X_0$ where the energy loss per unit length is $S_0 = 5.09\frac{\text{Mev}}{\text{cm}}$

and the radiation length is $X_0 = 8.9$ cm for aluminum. Thus, electron energies in the experiment do not deviate greatly from $E_{crit} = 45$ MeV.

Utilizing the geometry of the experiment, the number of muon decays at different radii is proportional to a geometric scaling factor of r. Meaning, the probability of a particular r is proportional to its own length. This can be visualized as a positive-linear probability distribution.

B. Simulation

For a selected value of $m_\mu c^2$, the simulation is executed 10,000 times. At each iteration, the quantities z_0, r, θ, Φ, and E_e are randomly chosen from the ranges $(0,\ t_p)$, $(0,\ \frac{R}{2})$, $(0,\ \theta_{max})$, $(0,\ 2\pi)$, and $(0,\ \frac{m_\mu c^2}{2})$, respectively. The probability distributions of z_0 and Φ are uniform. The quantity r has a positive-linear distribution and E_e has a distribution derived in [1] from the Fermi description of muon decay:

$$P(E_e) = C(m_\mu c^2 E_e)^2(3 - 4E_e/m_\mu c^2) \tag{2}$$

where C is a normalization constant to make the probability unity. With these random quantities, l and l_{esc} are computed from:

$$l = X_0 \ln\left[1 + \frac{E_e}{E_{crit}}\right] \tag{3}$$

$$l_{esc} = \frac{-r\cos\Phi + \sqrt{r^2\cos^2\Phi + (R^2 - r^2)}}{\sin\theta}\frac{t_p}{t_p + t_g}. \tag{4}$$

If the condition that $l > l_{esc}$ is satisfied, l is set to equal l_{esc}. Then, the number of sparks is calculated:

$$n_s = 1 + \text{floor}\left[\frac{l\cos\theta - z_0}{t_p}\right]. \tag{5}$$

To visualize the results of 10,000 iterations at a particular $m_\mu c^2$, a histogram is used with the bins representing n_s and the number of counts representing the number of muon decays, normalized to the total number of muon decays $N_{tot,exp} = 43$. Varying $m_\mu c^2$ with stepsize = 0.4 MeV, the χ^2 is computed:

$$\chi^2 = \sum_{n_s}\left[\frac{N_{sim}(n_s) - N_{exp}(n_s)}{\sigma_{exp}}\right]^2 \tag{6}$$

where the uncertainty σ_{exp} is the square root of the experimental counts $N_{exp}(n_s)$ as seen in Table I. The χ^2 results are fit to a parabola using 'numpy.polyfit', and the minimum of the fit represents χ^2_{min}.

C. θ Distributions

There are three θ distribution shapes tested which are uniform, triangular, and positive linear. The uniform distribution weighs all possible values of θ with equal probability, and was executed with θ_{max} at 30^o, then at 40^o. The triangular distribution has a probability which increases linearly from $\theta = 0^o$ to a peak at $\theta = 30^o$, then decreases linearly to zero probability at $\theta = \theta_{max} = 40^o$. Lastly, the positive linear distribution has a probability which increases linearly from zero probability to maximum probability at θ_{max}, and was executed with θ_{max} at 30^o, then at 40^o.

The idea behind these various distributions is that the reference [1] used a uniform distribution, but it would make more sense to use a different distribution. This is because there is more cylindrical volume that allows for larger angles to have greater probability. Due to the experimental limitations, θ_{max} was assumed 30^o in the reference [1] simulations. However, it was mentioned in their conclusions that increasing θ_{max} to 40^o produces results more similar to the accepted muon mass. Along with this, a probability cutoff at a particular angle does not physically make sense, but is a consequence of the . Thus, the triangular distribution was tested because its probabilities are bound to zero at both ends.

IV. RESULTS

The results of the five tests are summarized in Table 2. The values of $m_\mu c^2$ which are marked green represent values that are within the accepted muon mass value of 105.7 $\frac{\text{MeV}}{c^2}$. The values marked red are not within uncertainty of the accepted muon mass.

Trial	θ Distribution	θ_{max} (^{o})	$m_\mu c^2$ (MeV)	χ^2_{min}
1	Uniform	30	98.3 ± 5.6	0.25
2	Uniform	40	102.7 ± 6.5	1.15
3	Triangular	40	106.1 ± 6.8	0.64
4	Pos-Linear	30	101.9 ± 6.0	0.26
5	Pos-Linear	40	111.2 ± 7.9	1.42

TABLE II. Simulation results for various θ distributions and choices of θ_{max}.

In minimum chi-square estimation, the best set of parameters is determined as the parameters which make the χ^2 test statistic as small as possible. Referring to Table II, there are two θ distributions which produce the smallest χ^2_{min} values that are comparable to one another. Trial 1 has a Uniform θ distribution with $\theta_{max} = 30^o$, producing a χ^2_{min} of 0.25. Trial 4 has a positive linear θ distribution with $\theta_{max} = 30^o$, producing a χ^2_{min} of 0.26. Although both of their χ^2_{min} are small, only the Trial 4 distribution produced a muon mass result that is within uncertainty of the accepted muon mass. The χ^2 and the

histogram plots of Trial 4 results can be seen in Figures 3 and 4.

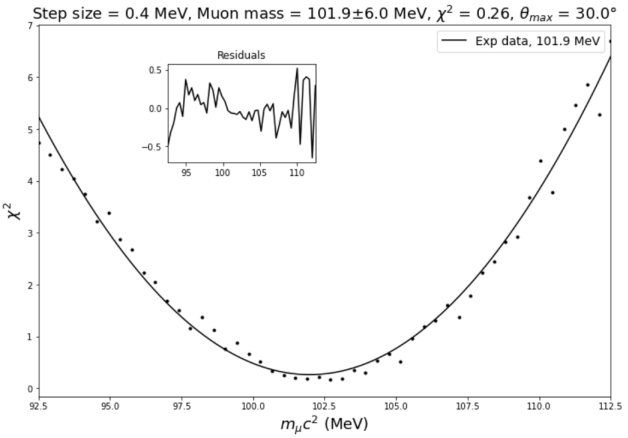

FIG. 3. Trial 4 plot of χ^2 versus $m_\mu c^2$. The residuals of the fit appear randomly distributed such that the quadratic fit is satisfactory for determination of the muon mass.

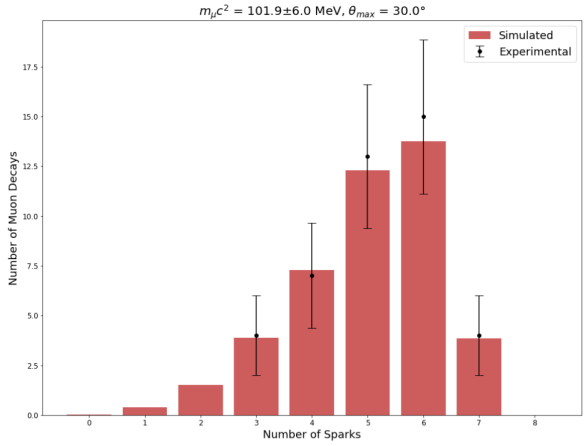

FIG. 4. Trial 4 histogram of the number of muon decays versus the number of sparks at the muon energy of 101.9 MeV, shown with the experimental data listed in Table I. All of the bin heights are in agreement with the experimental number of muon decays, such that taking the muon mass value at χ^2_{min} is justified.

A. Analysis

The simulation was written in Python using the Spyder IDE. After the simulation is run for the input range of $m_\mu c^2$ values, χ^2 is plotted against $m_\mu c^2$ with its quadratic fit and an superimposed plot of the fit residuals. From these results, the $m_\mu c^2$ corresponding to χ^2_{min} is deduced. The uncertainty is computed as the combined $\Delta_{m_\mu c^2}$ from the differences between $m_\mu c^2$ when χ^2_{min} is increased by the numeric value of one from the left (L) and right (R) sides from the $m_\mu c^2$ at χ^2_{min}. These differences are $\Delta_{m_\mu c^2,L}$ and $\Delta_{m_\mu c^2,R}$. They are added in quadrature and the square root is taken to deduce $\Delta_{m_\mu c^2}$, as seen in the equation:

$$\Delta_{m_\mu c^2} = \sqrt{(\Delta_{m_\mu c^2,L})^2 + (\Delta_{m_\mu c^2,R})^2}. \tag{7}$$

This calculation is allowed assuming that the uncertainty from the left and the uncertainty from the right are independent of one another and it also allows the larger uncertainty to be weighted more. Following this, the simulation is run once more to produce a histogram of the number of muon decays for the $m_\mu c^2$ at χ^2_{min}. This entire process is run a total of five times, each for a different distribution of θ. The reason why the simulation is run again is for efficiency purposes. Since, to store the data for the histogram $m_\mu c^2$ at χ^2_{min}, the data at every possible $m_\mu c^2$ would have needed to be saved prior. This is allowed because the shape of the histogram does not visually vary significantly between simulations, due to the high number of 10,000 iterations.

V. CONCLUSIONS

The aim of this experiment was to compute a more accurate muon mass value, compared to the accepted value of $105.7\frac{\text{MeV}}{c^2}$, than the reference [1] measurement of $100 \pm 5\frac{\text{MeV}}{c^2}$. When comparing the results of these simulations to the prior simulation, it is important to note the difference in the uncertainties. The calculation for the uncertainties in Table II was described in part D of section II. Unlike this method, the uncertainty in the referenced simulation was taken as the step size between the various tested values of muon mass. Thus, these uncertainties are computed differently and incomparable in magnitude.

The results of the simulations fulfilled the aim of the experiment. This is because four of the five trials fall within uncertainty of the accepted muon energy. This is better than the reference [1] result because their measurement of $100 \pm 5\frac{\text{MeV}}{c^2}$ did not fall within uncertainty of the muon mass. Based on the χ^2_{min} results described in section III, it is possible that the Trial 4 distribution, which yields a muon mass value of $101.9 \pm 6.0\frac{\text{MeV}}{c^2}$, is the best model for this simulation. However, it is important to note that Trials 2, 3, and 5 also produced more accurate results and their θ distributions are reasonable as well. Notably, the base value for the trial 3 result of $106.1 \pm 6.8\frac{\text{MeV}}{c^2}$ is closest to the accepted muon mass.

If this analysis were continued further, it would be good to compute the mean and standard deviations of many tests of the five distribution trials, in order to see what uncertainty is attributable to the 10,000 random sets of variables. Also, it would be interesting to test other θ distributions which are continuous and nonlinear.

VI. ACKNOWLEDGMENTS

We would like to express our sincere acknowledgement to our instructor, Dr. Chen Wang, for providing us the guidance and resources to be successful in this project.

VII. REFERENCES

[1] American Journal of Physics **78**, 64 (2010); doi: 10.1119/1.3230034